The role of projectile interactions in triply differential cross sections for excitation-ionization of helium

R. Dey[a,*] and A. C. Roy[b]

[a] *Max-Planck Institut für Plasmaphysik,*

Boltzmannstr. 2, D-85748 Garching, Germany

[b] *School of Mathematical Sciences, Ramakrishna Mission Vivekananda University,*

Belur Math 711202, West Bengal, India

Abstract

We report triply differential cross section (TDCS) for the simultaneous excitation-ionization of helium by electron impact for both coplanar and non-coplanar geometry. In the coplanar case, calculations have been performed for an incident energy of 500 eV and low ejection energies (3 eV and 10 eV), whereas in the noncoplanar case we have considered impact energies in the range 1240-4260 eV for a symmetric geometry. The present calculation is based on the eikonal approximation due to Glauber. We have incorporated the effect of post collision interaction in the Glauber approximation. A comparison is made of the present calculations with the results of other theoretical methods and recent experiments. The Glauber results are in reasonably good agreement with the experiment for small scattering angles.

PACS numbers: 34.50.Fa

Keywords: Triply differential cross section, Ionization-Excitation, Glauber approximation

* Correspondence author.

E-mail address: ritud@ipp.mpg.de (R. Dey)

Tel:00498932991884

1. INTRODUCTION

The study of excitation-ionization of helium by charged particle impact is of increasing interest because of the important role of correlation and higher-order interactions between the projectile and the target. Helium is the simplest target to study the above reaction process where one electron is ejected and the other is transferred to an empty orbital. It is noteworthy that in the absence of correlation the first Born amplitude vanishes in the case of above reaction process, although the higher terms of the Born series survives.

Over the last few decades, the ionization-excitation process has been extensively studied both theoretically and experimentally [1, 2]. Recently, Sakhelashvili et al [3] reported a triple-coincidence experiment for simultaneous ionization-excitation of helium for 500 eV electron impact. They have compared their relative experimental data with two different theoretical models, namely, momentum space close-coupling (CCC) and configuration space R-matrix with pseudostates (RMPS) and found the importance of accounting for second-order effects in the projectile-target interaction. Very recently, Harris et al [4] reported a new model, the four-body distorted wave (4DW) model to study the electron impact excitation-ionization process of helium. The 4DW model considers all projectile interactions including the initial- and final-state projectile-target interactions and the post-collision interaction between the two continuum electrons. They have compared their 4DW results with an otherwise equivalent first Born approximation (FBA) model and a second Born R-matrix pseudostates calculation (DWB2-RMPS). The above two models have mixed success for an incident energy of 500 eV and low ejection energies (3 eV and 10 eV).

Recently, Watanabe et al [5, 6] have studied simultaneous excitation-ionization processes of He by electron momentum spectroscopy (EMS). It is a powerful tool for investigating the electronic structure of matter. The kinematic variables that are measured for EMS are normally restricted to the vicinity of the Bethe ridge [7] i.e. at high impact energies and high momentum transfers. In [5], Watanabe et al reported the (e,2e) and (e,3-1e) experiments at an impact energy of 2080 eV in the symmetric noncoplanar geometry i.e. two outgoing electrons have equal scattering polar angles ($\theta_1 = \theta_2$=45^o) and energies (E_1=E_2). The measured momentum profiles were compared with the first-order plane-wave impulse approximation (PWIA) calculations using various ground state wave functions. In [6], the experiment was performed at incident energies of 1240 and 4260 eV for symmetric non-coplanar geometry.

Watanabe et al [6] have also reported second Born approximation (SBA) results and compared their theoretical cross sections with the measured data. Their calculations show a significant impact energy dependence and a clear evidence that higher order approximations beyond the first order plane wave impulse approximation are needed to explain the experimental data.

In the present paper we have concentrated on the study of the role of projectile interaction in the simultaneous excitation-ionization process by analysing the measurements of Sakhelashvili et al [3] as well as those of Watanabe et al [5, 6]. The effectiveness of different theoretical models are also assessed in reproducing the momentum profiles. In this work we have applied the eikonal approximation due to Glauber (GA) [8] which contains projectile-target correlation in the entrance channel. In fact, Glauber amplitude contains terms of all orders in V (i.e. the sum of projectile-core and projectile-electron interaction) in its phase. In the exit channel we have introduced the post collision interaction (PCI) effect, i.e., projectile-ejected electron correlation in the GA (GA-PCI) and studied the role of PCI using several wavefunctions.

The GA method has been successfully applied to a wide variety of atomic collisions [9–14]. Recently, we have applied this method to calculate TDCS for the single ionization of He where the residual ion is left in the $He^+(1s)$ state [13]. In the case of 1 KeV electron impact and ejection energy of 10 eV, GA was found to be reasonably satisfactory. In the present investigation we apply this method to the case of excitation-ionization of helium where correlation and higher order effects have very important roles.

2. THEORY

The Glauber amplitude for the ionization of helium by electron impact is given by (atomic units are used throughout, unless otherwise indicated) [15]

$$F(\mathbf{q},\mathbf{k_2}) = \frac{ik}{2\pi}\int d\mathbf{b}d\mathbf{r_1}d\mathbf{r_2}\phi_f^*(\mathbf{r_1},\mathbf{r_2})\Gamma(\mathbf{b},\mathbf{r_1},\mathbf{r_2})\phi_i(\mathbf{r_1},\mathbf{r_2})\exp(i\mathbf{q}.\mathbf{b}) \tag{1}$$

where

$$\Gamma(\mathbf{b},\mathbf{r_1},\mathbf{r_2}) = 1 - \left(\frac{\mid \mathbf{b}-\mathbf{s_1} \mid}{b}\right)^{2i\eta}\left(\frac{\mid \mathbf{b}-\mathbf{s_2} \mid}{b}\right)^{2i\eta} \tag{2}$$

$\mathbf{q}$=$\mathbf{k}$-$\mathbf{k_1}$ and η=1/k. Here $\mathbf{k}$, $\mathbf{k_1}$ and $\mathbf{k_2}$ are the momenta of the incident, scattered and ejected electrons, respectively. $\mathbf{b}$, $\mathbf{s_1}$ and $\mathbf{s_2}$ are the respective projections of the position vectors of the incident particles and the two bound electrons onto the plane perpendicular to the direction of the Glauber path integration. In equation (1), $\mathbf{q}$, $\mathbf{b}$, $\mathbf{s_1}$ and $\mathbf{s_2}$ are coplanar. $\phi_i(\mathbf{r_1}, \mathbf{r_2})$ and $\phi_f(\mathbf{r_1}, \mathbf{r_2})$ represent the wave functions of the initial and the final states of the target, respectively. For the initial state of helium, we have chosen three different wave functions. First, we have chosen the wave function given by Byron and Joachain [16] which is an analytic fit to the Hartree-Fock wave function:

$$\phi_{i,BJ}(\mathbf{r_1}, \mathbf{r_2}) = U(\mathbf{r_1})U(\mathbf{r_2}) \tag{3}$$

where

$$U(\mathbf{r}) = (4\pi)^{-1/2}(Ae^{-\alpha r} + Be^{-\beta r})$$
$$A = 2.60505 \qquad B = 2.08144 \qquad \alpha = 1.41 \qquad \beta = 2.61.$$

Secondly, the wave function considered is due to Hylleraas-Eckart-Chandrasekhar [17–19] with radial correlation:

$$\phi_{i,HEC}(\mathbf{r_1}, \mathbf{r_2}) = \frac{1}{\sqrt{N}}[\exp(-\alpha_1 r_1 - \beta_1 r_2) + \exp(-\alpha_1 r_2 - \beta_1 r_1)], \tag{4}$$

where N is the normalization coefficient and α_1=1.188530 and β_1=2.183171. Lastly, we have studied a simple configuration interaction wave function proposed by Silverman et al [20]:

$$\begin{aligned}\phi_{i,SIL}(\mathbf{r_1}, \mathbf{r_2}) &= (1+\lambda^2)^{-1/2}\{N[R'_{10}(\mathbf{r_1})Y_{00}(\mathbf{r_1})R_{10}(\mathbf{r_2})Y_{00}(\mathbf{r_2}) + R'_{10}(\mathbf{r_2})Y_{00}(\mathbf{r_2})R_{10}(\mathbf{r_1})Y_{00}(\mathbf{r_1})] \\ &+ \frac{\lambda}{3}[R_{21}(\mathbf{r_1})Y_{10}(\mathbf{r_1})R_{21}(\mathbf{r_2})Y_{10}(\mathbf{r_2}) + R_{21}(\mathbf{r_1})Y_{11}(\mathbf{r_1})R_{21}(\mathbf{r_2})Y_{1-1}(\mathbf{r_2}) \\ &+ R_{21}(\mathbf{r_1})Y_{1-1}(\mathbf{r_1})R_{21}(\mathbf{r_2})Y_{11}(\mathbf{r_2})]\}\end{aligned} \tag{5}$$

where

$$\lambda = -0.0617557, \qquad N = [2 + 2s^2(a,b)]^{-1/2} \qquad s(a,b) = 8[\frac{(ab)^{3/2}}{(a+b)^3}]. \tag{6}$$

The normalised radial portions are

$$\begin{aligned} R_{10} &= 2a^{3/2}\exp(-ar) \\ R'_{10} &= 2b^{3/2}\exp(-br) \\ R_{21} &= (2/\sqrt{3})g^{5/2}\exp(-gr) \end{aligned}$$

where a, b and g are the variationally determined orbital exponents. The final state wave function is made orthogonal to the ground state wave function in the following manner:

$$\Phi_f(\mathbf{r_1},\mathbf{r_2}) = \phi_f(\mathbf{r_1},\mathbf{r_2}) - S\phi_i(\mathbf{r_1},\mathbf{r_2}), \tag{7}$$

where,

$$S = \int \phi_f^*(\mathbf{r_1},\mathbf{r_2})\phi_i(\mathbf{r_1},\mathbf{r_2})d\mathbf{r_1}d\mathbf{r_2}, \tag{8}$$

and $\phi_f(\mathbf{r_1},\mathbf{r_2})$ is the symmetrised product of the hydrogenic wavefunction for the residual He^+ ion times a Coulomb wave. It is given by

$$\phi_f(\mathbf{r_1},\mathbf{r_2}) = 2^{-1/2}[\phi_{\mathbf{k_2}}(\mathbf{r_1})\nu_{nlm}(\mathbf{r_2}) + \nu_{nlm}(\mathbf{r_1})\phi_{\mathbf{k_2}}(\mathbf{r_2})] \tag{9}$$

where ν_{nlm} are the hydrogenic wave functions [21] and

$$\phi_{\mathbf{k_2}}(\mathbf{r}) = (2\pi)^{-3/2}exp(\frac{1}{2}\gamma\pi)\Gamma(1+i\gamma)exp(i\mathbf{k_2}.\mathbf{r})_1F_1(-i\gamma,1,-i(k_2r+\mathbf{k_2}.\mathbf{r})). \tag{10}$$

In Eq. (10) $\gamma = 1/k_2$. The triply differential cross section is given by

$$\frac{d^3\sigma}{d\hat{\mathbf{k}}_\mathbf{1}d\hat{\mathbf{k}}_\mathbf{2}dE_2} = \frac{k_1k_2}{k} \mid F(\mathbf{q},\mathbf{k_2}) \mid^2 \tag{11}$$

where we sum the TDCS contributions from all individual degenerate substates, since the measurements are unable to distinguish these substates of the ion. In Eq. (11) $d\hat{\mathbf{k}}_\mathbf{1}$ and $d\hat{\mathbf{k}}_\mathbf{2}$ denote, respectively, elements of solid angles of the scattered projectile and the ejected electron and dE_2 represents the energy interval of the ejected electron.

We have introduced the effect of PCI in the GA in the same way as was in [22] where the

PCI is introduced by multiplying the transition amplitude by a Coulomb factor proportional to $\mid v_e - v_p \mid^{-1}$ where v_e and v_p are the electron and projectile velocities respectively.

3. RESULTS AND DISCUSSION

Fig. 1 shows a comparison of present GA calculations with the relative experimental data [3] for 500 eV electron impact ionization of helium for the transition to the He^+(2p) state. In the present preliminary study, we have considered three simple wave functions, namely, $\phi_{i,BJ}$, $\phi_{i,HEC}$ and $\phi_{i,SIL}$ which correspond to ground state energies of -2.86167, -2.8756614 and -2.8952278 a.u., respectively for the initial target state of helium. Of these wave functions, $\phi_{i,SIL}$ yields the best ground state energy since the experimental value is -2.90372 a.u. Although the above wave functions are not highly correlated, the wave function of the initial state of the system considered in the present GA calculation takes into account both the projectile-electron correlation as well as projectile-target nucleus correlation. The calculations are performed for E_2=3 and 10 eV and θ_1=4.1 and 3.6^o. Harris et al [4] have normalised the experimental data to the binary peak of their 4DW calculation at E_2=3 eV and θ_1=4.1^o. For the sake of comparison, we have multiplied our GA results by appropriate factors (see the figure captions) to normalise them to the same point. In Fig. 1, we notice that the cross sections predicted by the GA-SIL and GA-BJ models agree more closely than those obtained by the GA-HEC methods especially in the angular region $180^o < \theta_2 < 260^o$. Although differing in detail the shapes of all the three curves are qualitatively the same. As the experimental data are relative we have calculated the ratio of binary and recoil peaks. TABLE I shows a summary of these ratios. A comparison with experiment shows that the ratios predicted by the GA-SIL model are better than those predicted by the GA-BJ method. Although GA-HEC ratio is inferior to GA-SIL results at E_2=3 eV, the former seems to be slightly better than the latter at ratio peaks at E_2=10 eV. This agreement is fortuitous, since in the neighbourhood of the recoil peak, GA-HEC overestimates the experimental data. Overall, GA-SIL appears to be the best of all the three wave functions considered in the present work.

Fig. 2 shows a comparison of present GA-SIL calculations of momentum profiles with those of the plane wave impulse approximation (PWIA), distorted wave Born approximation (DWBA), second-Born-approximation (SBA) and the experimental data [5, 6] at the incident

energy E=1240, 2080 and 4260 eV for electron impact ionization of helium for the transition to the n=2 state. The present calculation is performed in the symmetric non-coplanar geometry with angles θ_1=θ_2=45^o. The magnitude of the ion recoil momentum p is expressed by p=$\sqrt{(p_0 - \sqrt{2}p_1)^2 + [\sqrt{2}p_1 sin(\frac{\Delta\phi}{2})]^2}$ where $\Delta\phi = \phi_1 - \phi_2 - \pi$ is the out-of-plane azimuthal angle difference between the two outgoing electrons. p_0 and p_1 are the momenta of the incident and one of the outgoing electron, respectively. The PWIA (DWBA) results at E=1240, 2080 and 4260 eV are scaled by factors of 1.43, 1.31, and 1.21 (1.06, 1.02, and 1.01), respectively, as mentioned by Watanabe et al [6]. As the SIL wave function seems to be the best of all three wave functions considered in the present work we have presented momentum profiles with this wave function only. The GA-SIL results are multiplied by factors 1.5, 1.3 and 1.15 for E=1240, 2080 and 4260, respectively. We notice that GA-SIL results are in reasonably good agreement with the experimental data for all the above three impact energies. We have also noticed that the momentum profiles of GA-SIL are similar in shape as the SBA. However, all the theoretical models, namely, PWIA, DWBA, SBA and GA-SIL slightly deviate from the experimental data for the momentum of the residual ion beyond 1 a.u.

Figs. 3-5 depict GA-HEC, GA-BJ and GA-SIL results with and without the PCI factors, respectively. Also included in these figures are the 4DW results and the experimental data. A comparison of GA models with their corresponding models with PCI will reveal the interaction of the scattered projectile with the ejected electron. We find that PCI has a substantial contribution in both the binary and recoil regions. Furthermore, a comparison of present GA-PCI models with experiment shows that the introduction of PCI in the GA improves the binary to recoil peak ratio considerably. However, in the absence of absolute data we are not able to make a critical study of different magnitudes predicted by the different theoretical models considered in this work.

Fig. 6 exhibits the present GA-SIL-PCI results together with the 4DW calculations and the measured data. 4DW predicts that the recoil peaks are larger than its binary counterparts. On the contrary, GA-SIL-PCI yields recoil peaks smaller than the corresponding binary peaks and shows reasonably good agreement with experiment especially in the angular region $180^o < \theta_2 < 260^o$ for all the kinematics studied in the present investigation (also see TABLE II).

4. CONCLUSIONS

We have applied the Glauber method to calculate TDCS for the excitation-ionization of helium by electron impact for co-planar and non-coplanar geometry. In the coplanar case, calculations have been performed for ionization with excitation to He^+(2p) state at an incident energy of 500 eV and for low ejection energies (3 eV and 10 eV). We have studied the reaction process using three different wave functions, namely, Byron and Joachain (BJ), Hylleraas, Eckardt and Chandrasekhar (HEC), and Silverman (SIL) wave functions. It is seen that overall, cross sections predicted by SIL wave function agree better with experiment than those obtained using the other two wave functions. We find that the shapes of GA-SIL-PCI cross sections are in better accord with experiment than the 4DW calculations for the kinematics studied in the present investigation. Since the available experimental data are relative we have compared the ratios of binary peak/recoil peak and found that GA-SIL-PCI results are noticeably better than the corresponding 4DW cross sections. We have also studied the role of projectile-ejected electron correlation, i.e., the PCI effect in the final state. it is found that PCI improves the GA calculation and has a substantial contribution for the asymmetric geometry.

In the noncoplanar case we have studied momentum profiles at impact energies of 1240, 2080 and 4260 eV for the symmetric geometry. Here we find that GA-SIL results are in reasonably good agreement with the measured data for all the impact energies. Furthermore, we notice that the momentum profiles of GA-SIL are similar in nature as SBA and deviate from the experimental data for the momentum of the residual He^+(n=2) ion beyond 1 a.u.

ACKNOWLEDGMENTS

This research was supported by Max Planck Institute for Physics of Complex Systems (MPIPKS) on "Multiply Differential cross sections for the ionization of atoms by charged particle impact". One of the authors (A. C. Roy) would like to express his gratitude to MPIPKS for the hospitality provided to him during his stay at MPIPKS where part of the work was accomplished. Author Ritu Dey is grateful to Professor Arne Kallenbach for his

kind help.

[1] Pascale J. Marchalant, B. Rouvellou, J. Rasch, S. Rioul, Colm T. Whelan, A. Pochat, D. H. Madison, H. R. J. Walters, J. Phys.B 33 (2000) L749.

[2] S. Bellm, J. Lower, K. Bartschat, Phys. Rev. Lett. 96 (2006) 223201.

[3] G. Sakhelashvili, A. Dorn, C. Höhr, J. Ullrich, A. S. Kheifets, J. Lower, K. Bartschat, Phys. Rev. Lett. 95 (2005) 033201.

[4] A. L. Harris, M. Foster, Ciarán Ryan-Anderson, J. L. Peacher, D. H. Madison, J. Phys. B: At Mol Opt. Phys. 41 (2008) 135203.

[5] N. Watanabe, Y. Khajuria, M. Takahashi, Y. Udagawa, P. S. Vinitsky, Yu. V. Popov, O. Chuluunbaatar, K. A. Kouzakov, Phys. Rev. A. 72 (2005) 032705.

[6] N. Watanabe, M. Takahashi, Y. Udagawa, K. A. Kouzakov, Yu. V. Popov, Phys. Rev. A. 75 (2007) 052701.

[7] E. Weigold, I. E. McCarthy, Electron Momentum Spectroscopy (Kluwer Academic/Plenum Publishers, New York, 1999).

[8] R. J. Glauber, in: W. E. Brittin, et al (Eds), Lectures in the Theoretical Physics, Vol. I, Interscience New Work, 1959, p.315.

[9] A. B. Voitkiv, B. Najjari, J. Ullrich, J. Phys. B: At Mol Opt. Phys. 36 (2003) 2591 .

[10] R. Dey, A. C. Roy, Phys. Lett. A 332 (2004) 60.

[11] R. Dey, A. C. Roy, Phys. Lett. A 353 (2006) 341.

[12] R. Dey, A. C. Roy, C. D. Cappello, Nucl. Instr. and Meth. B 266 (2008) 242.

[13] R. Dey, A. C. Roy, Nucl. Instr. and Meth. B 267 (2009) 2357.

[14] M. Schulz, A.C. Laforge, K.N. Egodapitiya, J.S. Alexander, A. Hasan, M. F. Ciappina, A. C. Roy, R. Dey, A. Samolov, A. L. Godunov, Phys. Rev. A 81 (2010) 052705.

[15] A. C. Roy, A. K. Das, N. C. Sil, Phys. Rev. A 28 (1983) 181.

[16] F. W. Byron Jr, C. J. Joachain, Phys. Rev. 146 (1966) 1.

[17] E. A. Hylleraas, Z. Phys. 54 (1929) 347.

[18] C. Eckart, Phys. Rev. 36 (1930) 878.

[19] S. Chandrasekhar, Astrophys. J. 100 (1944) 176.

[20] J. N. Silverman, O. Platas, F. A. Matsen, The Journal of Chem. Phy. 32 (1960) 1402.

[21] B. H. Bransden, C.J. Joachain, in: Physics of Atoms and Molecules, 2nd edition, Prentice Hall (2003), p.160.

[22] A. Salin, J. Phys.B 2 (1969) 631.

Figure Captions:

Fig. 1: Triply differential cross section for ionization to He^+(n=2) at an impact energy of 500 eV. The solid curve represents the present GA calculation with BJ wave function. The dashed-dot curve represents the GA-SIL result. The dashed curve represents the GA-HEC result. The solid circles with error bars are the experimental data [3]. The GA-BJ, GA-SIL and GA-HEC results are multiplied by factors 2.17, 2.3 and 3.0, respectively for E_2=3 eV (θ_1=4.1^o). The GA-BJ, GA-SIL and GA-HEC results are multiplied by factors 1.4, 1.42 and 1.98, respectively for E_2=10 eV (θ_1=3.6^o).

Fig. 2: Triply differential cross section for the single ionization of helium by E=1240, 2080 and 4260 eV electron impact as a function of the momentum of the residual ion for the transition to the He^+(n=2). Here contributions from both the 2s and 2p states are included. The solid curve represents the GA-SIL results. The dotted curve represents the SBA [6] results. The dashed-dot curve represents the PWIA [6] results. The dashed curve represents the DWBA results [6].The solid circles with error bars are the experimental data [5,6]. The GA-SIL are multiplied by 1.5, 1.3 and 1.15 for E=1240, 2080 and 4260 eV respectively.

Fig. 3: Triply differential cross section for ionization to He^+(n=2) at an impact energy of 500 eV. The solid curve represents the present GA-HEC results. The dashed-dot curve represents the 4DW [4] result. The dotted curve represents the GA-HEC-PCI result. The solid circles with error bars are the experimental data [3].

Fig. 4: Triply differential cross section for ionization to He^+(n=2) at an impact energy of 500 eV. The solid curve represents the present GA-BJ results. The dashed-dot curve represents the 4DW [4] result. The dotted curve represents the GA-BJ-PCI result. The solid circles with error bars are the experimental data [3].

Fig. 5: Triply differential cross section for ionization to He^+(n=2) at an impact energy of 500 eV. The solid curve represents the present GA-SIL results. The dashed-dot curve represents the 4DW [4] result. The dotted curve represents the GA-SIL-PCI result. The

solid circles with error bars are the experimental data [3].

Fig. 6: Triply differential cross section for ionization to He^+(n=2) at an impact energy of 500 eV. The solid curve represents the present GA-SIL-PCI results. The dashed-dot curve represents the 4DW [4] result. The solid circles with error bars are the experimental data [3]. The GA-SIL-PCI results are multiplied by factors 1.32 and 0.76 for E_2=3 eV (θ_1=4.1^o) and 10 eV(θ_1=3.6^o), respectively.

Table Captions:

TABLE I: Comparison of binary to recoil peak ratio.

TABLE II: Comparison of binary to recoil peak ratio.

TABLE I: Comparison of binary to recoil peak ratio:

Peak ratio	GA-SIL	GA-HEC	GA-BJ	Expt. [3]
E_2=3 eV and θ_1=4.1^o	1.040	0.749	0.972	1.993
E_2=10 eV and θ_1=3.6^o	1.829	1.393	2.054	1.542

TABLE II: Comparison of binary to recoil peak ratio:

binary/recoil peak ratio	GA-SIL-PCI	4DW [4]	Expt. [3]
E_2=3 eV and θ_1=4.1^o	1.331	0.788	1.993
E_2=10 eV and θ_1=3.6^o	2.390	0.698	1.542

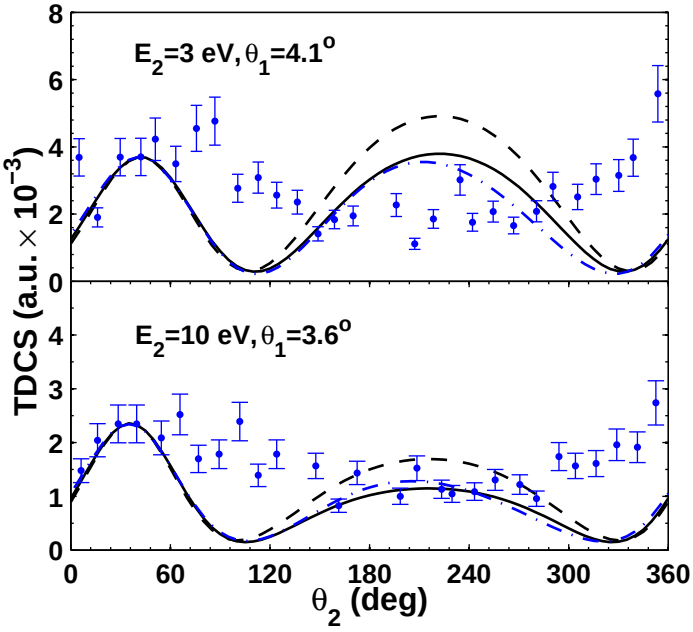
E2=3 eV, θ1=4.1°
E2=10 eV, θ1=3.6°
TDCS (a.u. × 10−3)
θ2 (deg)
0
60
120
180
240
300
360

Fig. 1

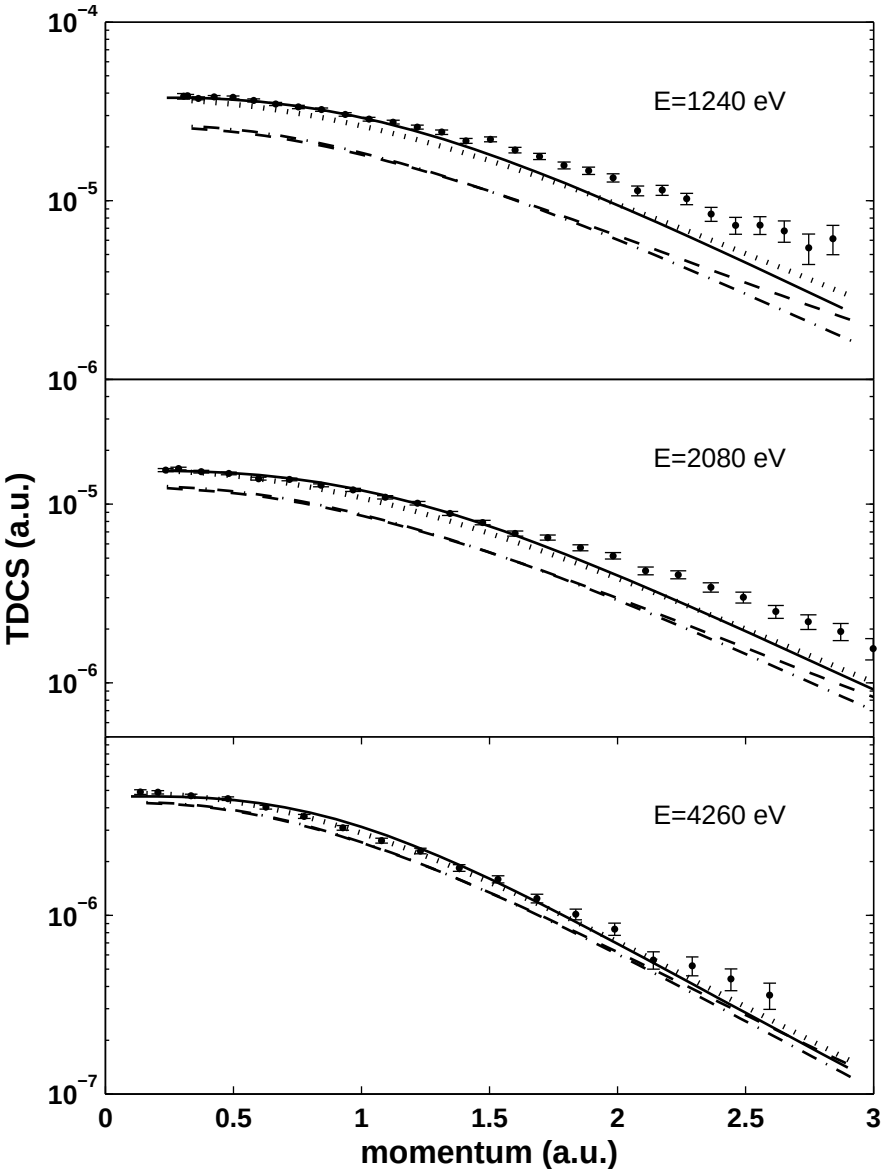
E=1240 eV
E=2080 eV
E=4260 eV
TDCS (a.u.)
momentum (a.u.)
10^-4
10^-5
10^-6
10^-7
0
0.5
1
1.5
2
2.5
3

Fig. 2

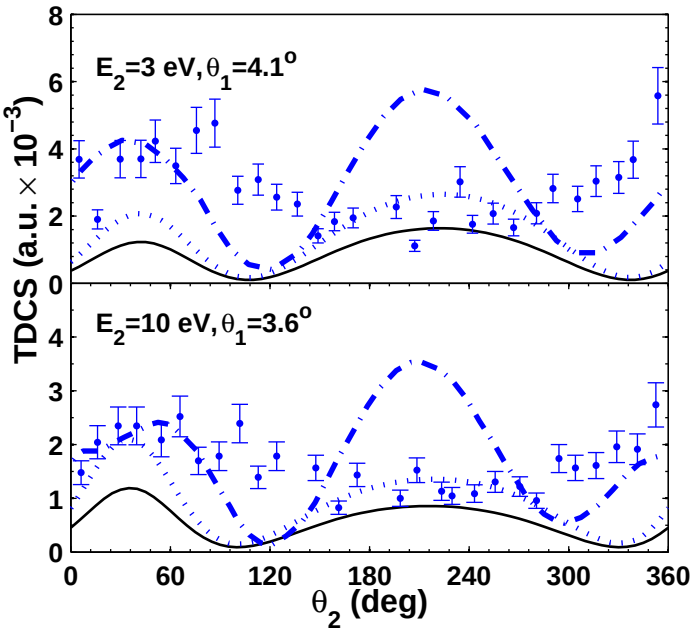
E2=3 eV, θ1=4.1°
E2=10 eV, θ1=3.6°
TDCS (a.u. × 10−3)
θ2 (deg)
0
60
120
180
240
300
360

Fig. 3

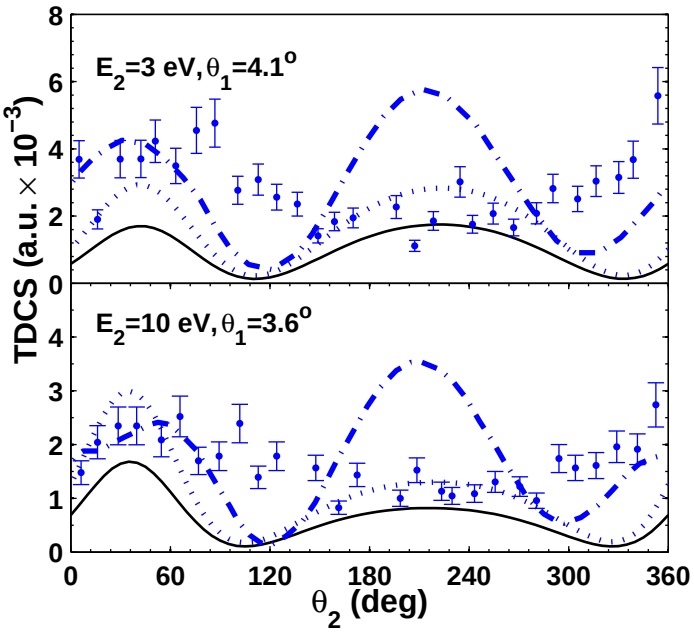
E2=3 eV, θ1=4.1°
E2=10 eV, θ1=3.6°
TDCS (a.u. × 10−3)
θ2 (deg)
0
60
120
180
240
300
360

Fig. 4

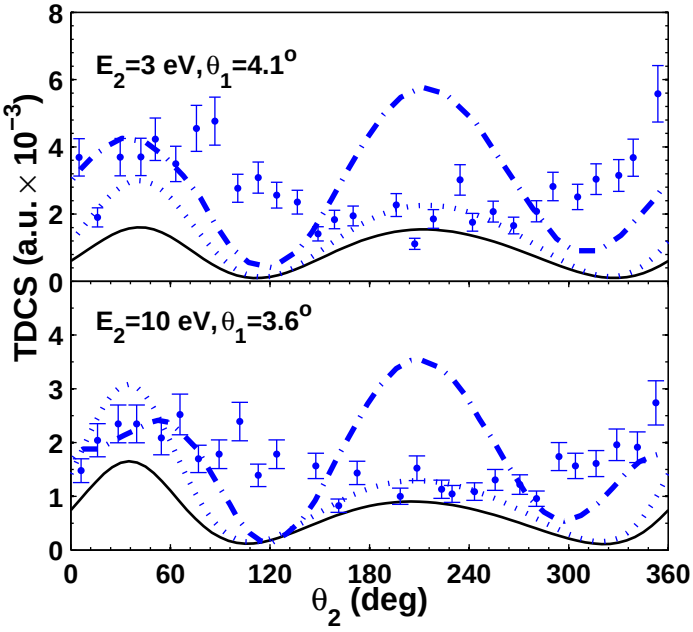
E2=3 eV, θ1=4.1°
E2=10 eV, θ1=3.6°
TDCS (a.u. × 10−3)
θ2 (deg)
0
60
120
180
240
300
360

Fig. 5

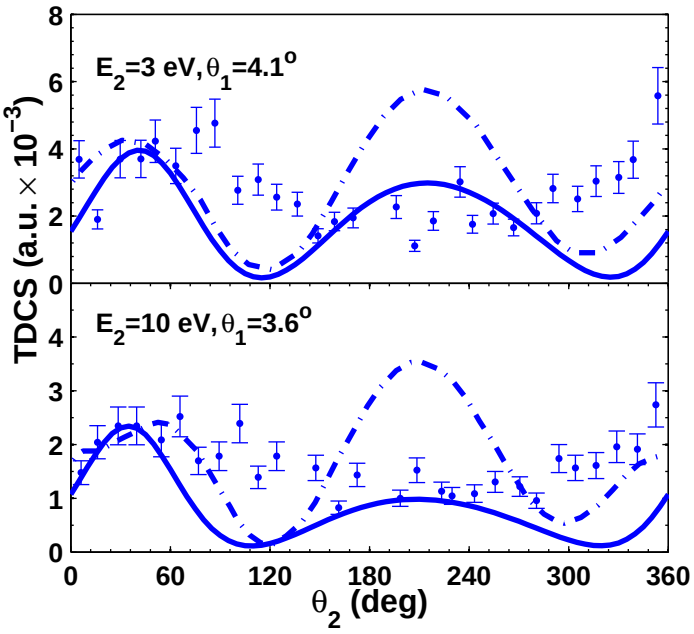
E2=3 eV, θ1=4.1°
E2=10 eV, θ1=3.6°
TDCS (a.u. × 10−3)
θ2 (deg)
0
60
120
180
240
300
360
0
2
4
6
8
0
1
2
3
4

Fig. 6